



Longitudinal Speed Control Using Model Reference Adaptive Control for Intelligent Highway Platform

Esmael Khanmirza ¹, Amid Maghsoudi ^{2*}, Farshad Gholami ³

¹ Assistant Professor, School of Mechanical Engineering, Iran University of Science and Technology, Tehran, Iran

² PhD. Candidate, School of Mechanical Engineering, Iran University of Science and Technology, Tehran, Iran

³ PhD. Candidate, School of Mechanical Engineering, Iran University of Science and Technology, Tehran, Iran

ARTICLE INFO

Article history:

Received :

Accepted:

Published:

Keywords:

Intelligent Highway

Intelligent Vehicle

Longitudinal Speed Control

Model Reference Adaptive

Control

A B S T R A C T

In the present study, the longitudinal dynamics control of intelligent vehicles in intelligent highway, in the presence of nonlinear factors, such as air resistance, rolling resistance, a not ideal gearbox, an internal combustion engine and a torque converter, is investigated. Moreover, considering the presented model and using model reference adaptive control, a proper controller is designed to control the longitudinal speed of intelligent vehicles. The results of the proposed model, which is validate by commercial software, are in good agreement with real-world situations. Hence, a positive step taken for controlling longitudinal speed of intelligent vehicles on an intelligent highway platform.

1. Introduction

Traffic control is a major and common problem in large-scale urban decision-making, particularly in metropolises. Several models of intelligent highways have been proposed to tackle the issue, and the longitudinal speed control of vehicles remains a key issue in the field of intelligent highways. Many researchers have been investigating the longitudinal speed control of vehicles. However, their proposed models disregard important and influential presumptions. Traffic management based on roadside control (including traffic signals, dynamic route information panels, dynamic speed limits, ramp metering, etc.). To promote the viewpoints concerning traffic control, new technologies in the field of communications and control are combined with current equipment and infrastructures [1]. This shows the advent of novel techniques in the field of traffic control and management, and a motivation to incorporate intelligent transportation systems or intelligent vehicle highway systems

(IVHS)[2]. IVHS is composed of three main parts: traffic management, driver information and vehicle control system, which would finally become automated highway system (AHS) by eliminating the driver [3]. Smart vehicles can also be classified into three main categories with respect to their dependence on the driver: 1. advisory system, 2. semi-autonomous, and 3. fully autonomous systems [4]. Current implemented traffic management systems are usually based on intelligent control by roadside infrastructure and do not benefit much from data obtained by intelligent vehicles. As a result, one of the methods for improving traffic management is using intelligent vehicles and taking advantage of data obtained from such vehicles. Finally, this has the benefit of making the movement of vehicles safer in such highways.

One of the most important issues by which comprehensive control of highways can achieve, is focusing on the management of vehicles having a close distance relative to each other. Such vehicles

* Amid Maghsoudi

Email Address: maghsoudi_amid@mecheng.iust.ac.ir

<https://doi.org/10.22068/ase.2019.399>

are called intelligent platoons [5]. In each vehicle platoon, the first vehicle calls platoon leader and others are followers. In this method, to avoid crashes, it is assumed that the distance between cars is larger than their dimensions [6]. Many researchers have considered the interconnection between vehicles as platoons and roadside infrastructure [7-9].

Adaptive cruise control systems are control systems based on the data obtained from radars. The obstacle identification functions by estimating the relative velocity between the vehicle and the obstacle. If the relative velocity is a small number, the obstacles considered as vehicles, and if the relative velocity is close enough to the vehicle speed, the obstacles consider stationary obstacle. Implementing the adaptive cruise control system at low velocities is problematic. Therefore, the stop-go model employs in this velocity range. In short, it can claim that in this type of controller, the control action applied on distance instead of velocity. Although the adaptive cruise control (ACC) system is reliable in most situations [10-11], it fails to correctly detect the front vehicle position in conditions such as the reduction of the next car velocity. Cooperative adaptive cruise control is the next and optimized version of adaptive cruise control that obtains data about braking or accelerating and maneuvering of vehicles from the network and immediately attempts to control the intelligent highway. It should be mentioned that this type of controller does not have a long history [12-16]

The first step in implementing the cruise control is controlling the longitudinal speed. Several researchers have attempted at controlling the longitudinal speed, among whom some have tried to use model-free approaches to eliminate modeling complexities. For instance, Menhour et al. controlled a Peugeot 406 using a model-free control method and the presented intelligent controller [17]. In addition, Zhang et al. developed a robust gain-scheduling approach to tackle the nonlinear effects of vehicle dynamics [18]. As can be noted, uncertainties and variation in vehicle dynamics is among the important issues in recent studies and researchers have been trying to present controllers capable of tackling unknown factors and with a design that is independent of known dynamics.

In previous studies, assumptions such as rolling resistance, air resistance, existence of a not ideal gearbox, the presence of a torque converter and an internal combustion engine are neglected. In this study, however, the researchers have tried to show the importance of the mentioned factors by

examining them, and could finally present a model reference adaptive controller (MRAC) for the system while noting the governing dynamics of the system and the variable nature of vehicle dynamics (engine behavior alteration, etc.). The results of this study, validated by commercial software, show the consistency between the proposed model and real-world cases. Hence, a positive step is taken for longitudinal speed control of intelligent vehicles on an intelligent highway platform.

In the first section, resistance forces related to vehicles discussed. Then, longitudinal dynamics in presence of resistance forces considered. In the equivalent mass and force section, all of the inertia and forces modeled after that, torque convertor explained. In the verification section, chosen dynamics of system verified then, the adaptive controller that is suitable for the equation has introduced. In the result section, the outputs are discussed.

2. Governing Equations

First, the significant forces acting on the vehicle in longitudinal motion investigated and then, the vehicle dynamics expounded.

2.1. Resistance forces

Rolling resistance: When the wheel is in the stationary state, the pressure distribution between the wheel and the ground is symmetric with respect to the tire contact point with the ground. When the vehicle is moving, however, the equivalent force exerted on the wheel by the ground is slightly shifted forward, owing to the disruption to the pressure distribution between the tire and the ground, which results in imposing a torque opposing the motion of the wheel, equal to Equation **Error! Reference source not found.** This phenomenon represented in Figure 1. In the picture stress distribution is shown by σ_z and equivalent concentrated force by F_z . The resisting force to the motion is defined, using the SAE standard and J670e data, as the force exerted on the wheel center [19]. In the following M_y is rolling resistance, F_z is equivalent normal force, Δx distance between equivalent normal force and the vertical axis.

$$M_y = -F_z \Delta x \quad (1)$$

This resisting torque is not practically described by, but the value of Δx is estimated through considering the effective radius as R_r , presenting

the rolling resistance as EquationError! Reference source not found. and calculating F_x via experimental methods and fitting it with the EquationError! Reference source not found.. It is important to note that in the equation Error! Reference source not found. and Error! Reference source not found., F_x is equivalent force that produce equivalent rolling resistance torque, f_i are constants which are achieved after curve fitting of experimental data with theory, u^i is longitudinal velocity to power (i). If rolling resistance force is for the front axis, F_x has index 1 and if F_x has index 2 it is for rare axis in the following equations.

$$M_y = -F_x R_r \tag{2}$$

$$F_x = f_r \times F_z \text{ and } f_r = \sum_{i=0}^n f_i u^i \tag{3}$$

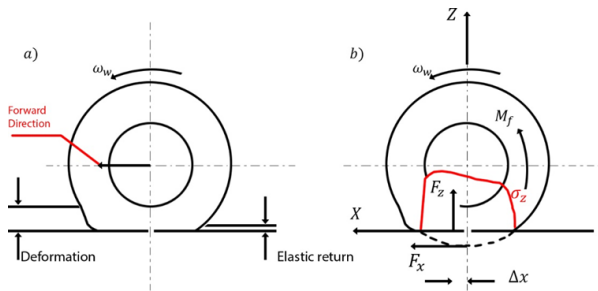


Figure 1. Pressure distribution between the tire and the ground, and the resulted deformation[20].

Air resistance force: In this study, air resistance has been considered as an influential force on the vehicle behavior and it was shown that it plays a significant role on the vehicle speed; emphasizing the importance of considering air resistance in modeling and vehicle control. To apply air resistance force in vehicle dynamics, EquationError! Reference source not found. has been utilized[20].

$$F_{aero} = \frac{1}{2} \rho_{air} S C_x u^2 \tag{4}$$

In which, ρ_{air} is the air density, S is the effective area at the front of vehicle, C_x is the air resistance constant and u is the longitudinal speed of the vehicle.

2.2. Longitudinal dynamics

Now, the forces acting on the vehicle axle should calculate and the acceleration must compute using the Newton's second law. The importance of this procedure lies in the fact that vehicle speed,

position, and other important parameters can be investigated. Since the forces acting on the vehicle applied in different manners due to their nature, and as they do not act on the vehicle mass center exactly, some moments created. Significant forces and parameters of vehicle longitudinal motion depicted in Figure 2,

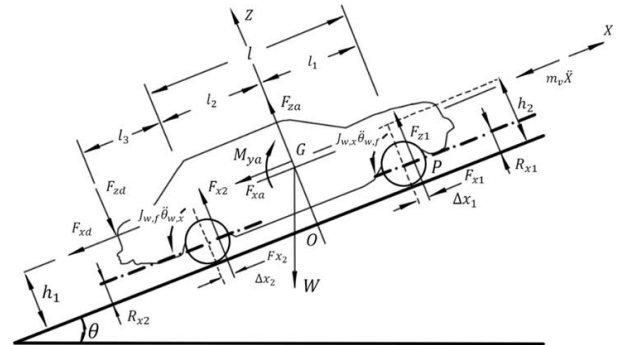


Figure 2. Forces acting on the vehicle in longitudinal motion[20]

in which, W is the weight force acting on the vehicle mass center, having two perpendicular components, one of which is in the direction of the inclined surface and the other perpendicular to the inclined surface. This type of decomposition can simplify the process of writing the equations of motion for the rest of the article. Moreover, m_v is vehicle mass, J_{wr} and J_{wf} are inertias of, respectively, the front and rear wheels, $\frac{d^2x}{dt^2}$ is the linear acceleration of the vehicle in the longitudinal direction of motion, $\theta_{w,f}$ and $\theta_{w,r}$ are rotation of front and rare wheels respectively and they will show by θ_w . $\frac{d^2\theta_f}{dt^2}$ and $\frac{d^2\theta_r}{dt^2}$ are rotational accelerations of, respectively, the front and rear wheels about the rotation axis of the wheels (y), l is the distance between the rotation axis of front and rear wheels, l_1 and l_2 are the distances from the mass center to the rotation axis of front and rear wheels, l_3 is the distance from vertical drawbar load and rear axle. In addition, F_{za} , F_{xa} and M_{ya} are, respectively, aerodynamic forces and moment acting on the vehicle body. F_{xa} is the aerodynamic force acting in x direction and can be considered as a concentrated force acting at a height of h_2 and causing the aerodynamic moment as EquationError! Reference source not found., and F_{za} is the aerodynamic force acting on the vehicle in z direction[20].

$$M_{ya} = F_{xa} h_2 \tag{5}$$

Where h_1 and h_2 are the distances between the road and the line of action of inertial force and

aerodynamic forces. Δx_1 and Δx_2 are, respectively, the distances between the line of action of vertical force exerting from the ground on the wheel and the center of front and rear wheels. F_{xd} And F_{zd} are, respectively, the horizontal and vertical forces acting on the tow bar handle from towing trailer.

To calculate the vertical force between the two wheels' axles and the ground, two equations are necessary. Noting Figure 2 and the described notation, and taking the moment about the point p , one of the equations described as

$$m_v \ddot{x} + 2J_{w.f} \ddot{\theta}_{w.f} + 2J_{w.r} \ddot{\theta}_{w.r} - 2F_{z2} \times (l_1 + \Delta x_1 - \Delta x_2) + F_{zd}(l + l_3 + \Delta x_1) + F_{xd}h_1 + F_{xa}h_2 - F_{za}(l_1 + \Delta x_1) - M_{ya} + W_x h_1 + W_z(l_1 + \Delta x_1) = 0 \quad (6)$$

For simplification, it is assumed that

$$M_{ya} = 0 \quad (7)$$

$$F_{za} = 0$$

Additionally, the forces from the tow bar on the vehicle ignored ($F_{xd} = 0$ and $F_{zd} = 0$). If the second moment of inertia of rear and front wheels and also their specifications and rotation value are considered equal, i.e.

$$J_{w.f} = J_{w.r} = J_w \quad (8)$$

$$\Delta x_1 = \Delta x_2 = U$$

$$\theta_{w.f} = \theta_{w.r} = \theta_w$$

And the equilibrium equation about the point p is rewritten, the following equation is obtained

$$m_v \ddot{x}h_1 + 4J_w \ddot{\theta}_w - 2F_{z2} l + F_{xa} h_2 + W_x h_1 + W_z(l_1 + U) = 0 \quad (9)$$

Where W_x and W_z are components in the direction of and perpendicular to the road, which can be written according to Equation Error! Reference source not found.. Here, F_{z1} and F_{z2} are normal forces related to front and rare axes respectively.

$$W_x = m_v g \sin(\Theta) = m_v gi \quad (10)$$

$$W_z = m_v g \cos(\Theta) = m_v g$$

Therefore, according to Equation Error! Reference source not found., the force

perpendicular to the inclined surface exerting on the rear wheel, can be described as

$$F_{z2} = \frac{1}{2} [m_v \ddot{x}h_1 + 4J_w \ddot{\theta}_w + F_{xa} h_2 + m_v gih_1 + m_v g(l_1 + U)] \quad (11)$$

To calculate the force perpendicular to the inclined surface exerting on the front axis, the equilibrium equation in the direction of the surface used,

$$F_{z1} = \frac{m_v g - 2F_{z2}}{2} \quad (12)$$

Therefore, the two equations by which the vertical forces acting on the axes estimated written as

$$F_{z1} = F_{z1}^s - \frac{1}{2l} [m_v \ddot{x}h_1 + 4J_w \ddot{\theta}_w + \dots + F_{xa} h_2 + m_v gih_1 + m_v gU] \quad (13)$$

$$F_{z2} = F_{z2}^s + \frac{1}{2l} [m_v \ddot{x}h_1 + 4J_w \ddot{\theta}_w + F_{xa} h_2 + m_v gih_1 + m_v gU] \quad (14)$$

In which F_{z1}^s and F_{z2}^s depict the static loading force estimable from Equation Error! Reference source not found.,

$$F_{z1}^s = \frac{m_v gl_2}{2l} \quad (15)$$

$$F_{z2}^s = \frac{m_v gl_1}{2l}$$

To determine the magnitude of exerted forces on the vehicle, two other equations are necessary. Therefore, these equations written for a vehicle with one drive shaft with the aid of Figure3.

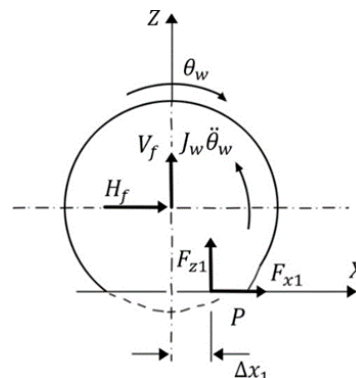


Figure 3. General forces acting on the front wheel[20].

Writing the equilibrium equation for the front axle about its center of rotation, results in Equation(16). It should note that in this study, the drive shaft taken as the rear axis,

$$J_w \ddot{\theta}_w + F_{1z}U + F_{x1}R_r = 0 \quad (16)$$

Likewise, another equation for rear axle wheels can be obtained as Equation(17).

$$F_{x2} = F_{x1} + \frac{1}{2}(m_v \ddot{x} + F_{xa} + m_v g i) \quad (17)$$

In figure 3, V_f and H_f are, respectively, the horizontal and vertical forces exerted on the wheel from the chassis. In the fowling, these two forces omitted because of being internal forces.

As some of the equations include angular velocity and acceleration, and some others involve the variables of linear velocity and acceleration of the vehicle, alongside the fact that in order to deal with a few number of variables, they should define in terms of one another, these variables presented as follows

$$\begin{aligned} u = \dot{x} &= \frac{\omega_{o.t} R_r}{\tau_c \tau_d} \\ a_x = \ddot{x} &= \frac{\dot{\omega}_{o.t} R_r}{\tau_c \tau_d} \\ \ddot{\theta}_w = \frac{\ddot{x}}{R_r} &= \frac{\dot{\omega}_{o.t}}{\tau_c \tau_d} \end{aligned} \quad (18)$$

Where τ_c and τ_d are, respectively, the transmission ratios (the ratio of output to input velocity) of the gearbox and final drive. In the gearbox, the gearshifts and for each gear, the transmission ratio and efficiency of the gearbox changes (the effect of gearbox transmission efficiency and final drive will consider in next sections). Furthermore, $\omega_{o.t}$ and $\dot{\omega}_{o.t}$ are, respectively, the rotational velocity and acceleration of the torque converter's output shaft.

It should be mentioned that a criterion was considered for shifting: when the engine RPM exceeds 5000 RPM, the gear shifts up and when the engine RPM drops below 2000 RPM, the gear shifts down.

In this study, to simplify matters, the vehicle mass and rotational inertia of the wheel in addition to the forces resisting the motion (rolling resistance, air resistance) equalized on an equal rotational inertia. Figure 4 is a representation of this equalization.

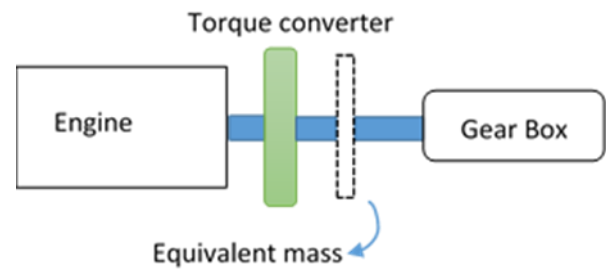


Figure 4. Representation of the equivalent mass equalization

2.3. Equivalent Mass and force

In this section, the equalization method of resistive forces in addition to the equivalent mass are studied. When the gearbox is ideal, the input power is equal to the output power (neglecting the rotational inertia of gears). In fact, in reality the output power is a fraction of the input power and since in the path of force transmission to the equivalent mass, there exists the gearbox and also a gear in the transmission line, the influence of efficiency should be considered at these two locations. In this study, η_c and η_d show the transmission efficiencies of gearbox and torque drive line, respectively. This leads us to the following equations,

$$\begin{aligned} T_{r.aero} d\theta_{o.t} &= F_{aero} ds \times \eta_c \eta_d \\ T_{r.aero} \frac{d\theta_{o.t}}{dt} &= F_{aero} \frac{ds}{dt} \times \eta_c \eta_d \\ T_{r.aero} \omega_{o.t} &= F_{aero} u \times \eta_c \eta_d \\ T_{r.aero} &= F_{aero} \frac{u}{\omega_{o.t}} \times \eta_c \eta_d \end{aligned} \quad (19)$$

Finally, considering Equations(18) and(19), we can obtained $T_{r.aero}$ in Equation (20) as following:

$$\begin{aligned} T_{r.aero} &= F_{aero} R_r \times \frac{\eta_c \eta_d}{\tau_c \tau_d} \\ &= \frac{1}{2} \rho_{air} S C_x u^2 R_r \times \frac{\eta_c \eta_d}{\tau_c \tau_d} \\ &= \frac{1}{2} \rho_{air} S C_x R_r^3 \frac{\omega_{o.t}^2 \eta_c \eta_d}{(\tau_c \tau_d)^3} \end{aligned} \quad (20)$$

In the same way, for the reduced torque caused by rolling resistance ($T_{r.rolling}$) and slope of ground($T_{r.slope}$):

$$\begin{aligned}
 T_{r.rolling} &= F_{rolling}R_r \times \frac{\eta_c \eta_d}{\tau_c \tau_d} \\
 &= F_z f_r R_r \times \frac{\eta_c \eta_d}{\tau_c \tau_d} \\
 T_{r.slope} &= F_{slope}R_r \times \frac{\eta_c \eta_d}{\tau_c \tau_d} \\
 &= W_i R_r \times \frac{\eta_c \eta_d}{\tau_c \tau_d}
 \end{aligned}
 \tag{21}$$

Moreover, to transmit inertia, the kinetic energy of each body should equalize with its equivalent mass. If the mass m_v and translational speed of u are assumed, and equivalent inertia in a rotational system with the rotational speed of $\omega_{o.t}$ is desired, then:

$$\begin{aligned}
 \frac{1}{2} m_v u^2 &= \frac{1}{2} I_e \omega_{o.t}^2 \\
 I_{e.v} &= m_v \left(\frac{u}{\omega_{o.t}} \right)^2 = m_v \left(\frac{R_r}{\tau_c \tau_d} \right)^2
 \end{aligned}
 \tag{22}$$

In addition, for the transmission of wheel inertia (I_w),

$$\begin{aligned}
 \frac{1}{2} I_w \omega_w^2 &= \frac{1}{2} I_e \omega_{o.t}^2 \\
 I_{e.w} &= I_w \left(\frac{\omega_w}{\omega_{o.t}} \right)^2 = I_w \left(\frac{1}{\tau_c \tau_d} \right)^2
 \end{aligned}
 \tag{23}$$

Now, knowing the reduced torques and equivalent mass, the next equation obtained as

$$\begin{aligned}
 T_{o.t} - T_{r.aero} - T_{r.rolling} - T_{r.slope} \\
 = (I_{e.v} + 4I_{e.w}) \dot{\omega}_{o.t}
 \end{aligned}
 \tag{24}$$

To calculate the above equation, the term $T_{o.t}$, which represents the output torque of the torque converter, should evaluate. The engine considered in this study is of the internal combustion type and the produced torque depends on the engine RPM and throttle. Figure 5 depicts the produced torque by this engine[20].

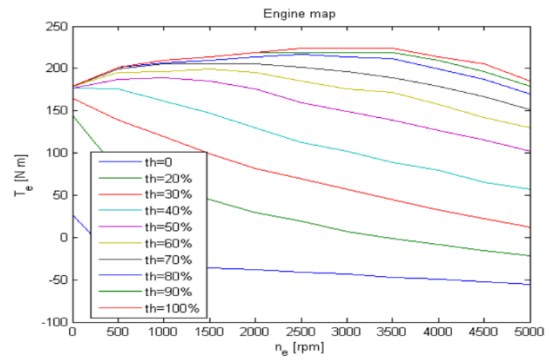


Figure 5. Diagram of the engine output torque with respect to the engine RPM and throttle

The engine output torque delivers to the torque converter and finally, a torque from the converter applies on the equivalent inertia.

2.4. Torque converter

Based on the rotational speed of engine and turbine (output of torque converter), the input and output moments of torque converter can be formulated as follows. First, the rotational speeds of either side of the torque converter should be calculated, as the amount of torque transmitted by the torque converter is dependent on the speed of its sides. To calculate the rotational speed of converter's input blade, Equation(25) should be utilized:

$$T_e - T_{t.i} = I_{e.i} \dot{N}_e
 \tag{25}$$

Where

- T_e and $T_{t.i}$ are, respectively, engine torque and input torque of engine
- $I_{e.i}$ represent rotational inertia of internal parts of engine, flywheel and torque converter's turbine
- N_e depicts rotational speed of engine (RPM)

The amount of torque converter output moment, noting the rotational speed of converter sides obtained via the following relations:

$$\begin{aligned}
 T_{t.i} &= \left(\frac{N_e}{K} \right)^2 \\
 K &= F_2 \left(\frac{N_{t.o}}{N_e} \right) \\
 R_{TQ} &= F_3 \left(\frac{N_{t.o}}{N_e} \right)
 \end{aligned}
 \tag{26}$$

In which $N_{t.o}$ is the output rotational speed of torque converter (RPM), equal to $N_{t.o} = \omega_{t.o} \times \frac{60}{2\pi}$, and R_{TQ} is the transmitted torque ratio. As shown in Equation(26), the torque ratio transmitted by the torque converter depends on two constants. These two constants can be found in CarSim software as functions of speed ratio for different types of torque converters. In this study, the available data for a Sedan car in the software has been used, similar to Ref[20]. A view of changes of these two constants can be seen in Figures 6 and 7.

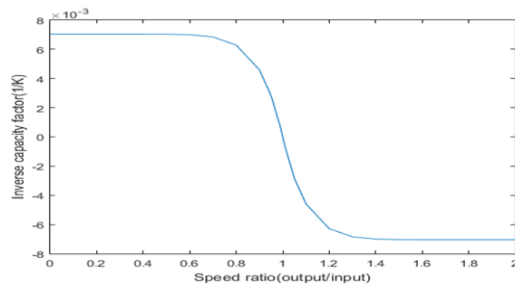


Figure 6. A view of inverse capacity factor (1/K) vs. speed ratio[21]

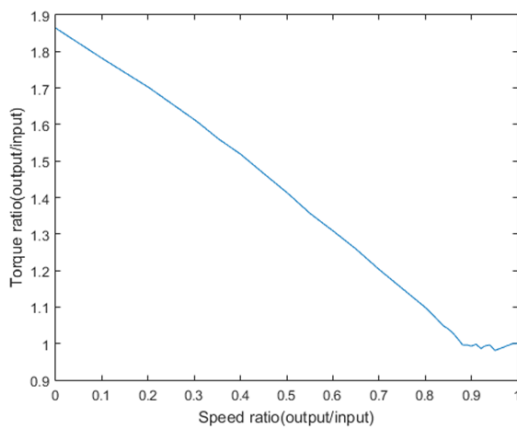


Figure 7. A view transmitted torque ratio vs. speed ratio[21].

3. Dynamics verification

All of the equations in this research have simulated in Matlab software and its Simulink part. Each simulation step has been verified with CarSim software with the parameter mentioned in reference[20]. Last validation result represented in Figure 9. The verification steps presented in Appendix. To verify the created model in the software, the commercial software, CarSim, is used in which longitudinal and lateral vehicle dynamics can be investigated by considering different parts of the vehicle such as engine, gearbox, tire, wind,

and other specifications. The throttle is set on semi-open state (50%) as the test condition. As can be seen in Figure 9, the simulated longitudinal dynamics is fully consistent with the results obtained from CarSim.

Sedan C class is used in CarSim and parameters in reference[20] are implemented. Figure 8 represents the CarSim environment that we enter the parameters.

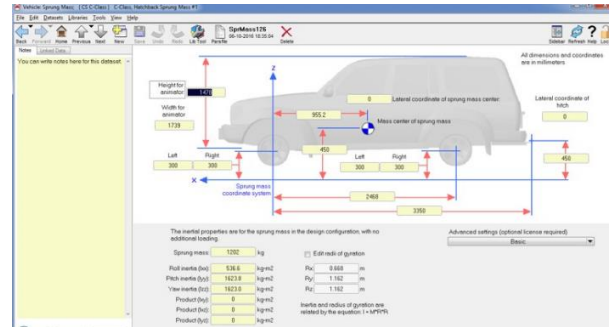


Figure 8.Importing data into CarSim software.

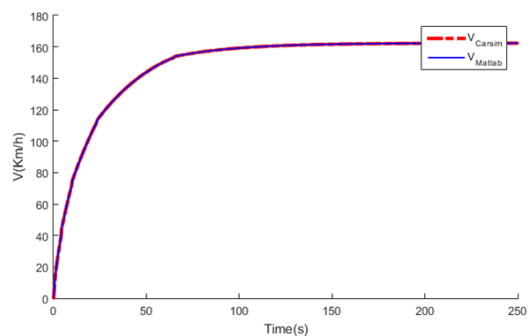


Figure 9. Longitudinal dynamics verification using the commercial software CarSim

4. Adaptive controller

As previously stated, the change in the behavior of vehicle at various moments and the change of parameters such as mass and other physical specifications force us to consider a controller capable of adapting itself to changeable circumstances. Consequently, the researchers have tried to implement this controller.

Model reference adaptive system (MRAS) is one of the most important adaptive controllers. In this controller, a stable system consider as a reference model, which is desire of control designer. Meanwhile, some terms exist in the input of the controller updated as time passes and converges the plant behavior to that of the reference model. Figure 10 shows a representation of the controlling process in this type of controller.

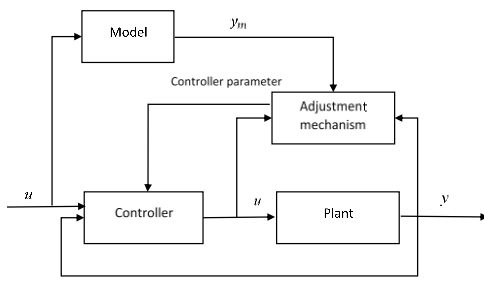


Figure 10. Model reference adaptive system (MRAS)[22].

Parameter adjustment in this method achieved by the two approaches of 1) gradient-based, and 2) application of Lyapunov stability theorem. In this study, parameter updating is attained by the method presented in Ref[22] and considering Lyapunov stability theorem. The governing equations of this method for the control of a linear system described in the state-space is presented in the following section.

Let the considered system be described according to Equation(27) and the desired system according to Equation(28),

$$\frac{dx}{dt} = Ax + Bu \tag{27}$$

$$y = Cx + Du$$

$$\frac{dx}{dt} = A_m x + B_m u \tag{28}$$

$$y_m = C_m x + D_m u$$

And the controller input as Equation(29),

$$u_{s \times 1} = k(t)_{s \times p} x_{p \times 1} + K_{r_{s \times s}} r_{s \times 1} \tag{29}$$

It is noteworthy that in Equation(29), s is the number of system inputs, and p is the number of system state. The parameters inside these two matrices constituting the vector θ will update according to Lyapunov stability theorem. The updating procedure of these parameters is reported to be as in Equation(30):

$$\dot{\theta} = -\Gamma \phi e^T P B \tag{30}$$

Where $\phi = [x^T \cdot r^T]^T$, Γ is a square matrix with the same length as the vector θ , and P is positive-definite matrix with the same dimension as the matrix B .

As can be seen, this type of controller is designed with the assumption of the system being linear, but

it can further be utilized for nonlinear systems such as vehicle dynamics noting the following explanations.

In this study, the dynamics of the vehicle has been considered similar to a linear system as in Equation(27). However, the matrix A is not constant and is a function of time. Furthermore, as the changes of this matrix does not happen rapidly and there is enough time for the controller to update, it has the ability of adapting itself to the circumstances surrounding the controller. Then, using the assumption gained by understanding vehicle dynamics and controller type, control of vehicle longitudinal speed considering the existence of nonlinear factors such as gear shifting, not ideal gearbox, air resistance, wheel rolling resistance, the presence of torque converter and internal combustion engine is represented. So, the high efficient controller for controlling such a complicated problem with nonlinear elements is introduced.

5. Results

In this section, the obtained results are presented. First, to show the importance of the preliminary assumptions in studying vehicle dynamics, some simulations are performed whose results are in Figure 11. All of these comparative simulations conducted with a 50% throttle. These assumptions, as mentioned in the beginning of the article consider the gearbox as its imperfect mechanism, in addition to considering rolling resistance and air resistance. The simulation was first performed with none of the above-mentioned items (dotted curve) after which the effect of gearbox as a non-ideal part is taken into consideration (dotted-line curve) and then the effect of air resistance is looked upon in the ideal model (dashed curve). Finally, the effect of rolling resistance and air resistance simultaneously applied on the ideal gearbox model. As evident, the proposed model is in good agreement with the real model, which shows the importance of the above parameters on the simulation and control of the model.

It should be mentioned that the influential parameters of performed simulations are determined using Ref[20], according to Table 1.

Table 1: Specifications of simulation [20].

Parameter	Value	Parameter	Value
m_v	1362 (kg)	l	2.47 (m)
l_1	0.95 (m)	l_2	1.51 (m)
$\eta_{c.1}$	0.80	$\tau_{c.1}$	3.73
$\eta_{c.2}$	0.91	$\tau_{c.2}$	2.05
$\eta_{c.3}$	0.93	$\tau_{c.3}$	1.32
$\eta_{c.4}$	0.92	$\tau_{c.4}$	0.97
η_d	0.80	τ_d	3.80
R_r	0.30	S	1.93 (m^2)
C_x	0.33	h_1, h_2	0.45 (m)
$I_{e.i}$	0.31 ($kg\ m^2$)	I_w	0.0069 ($kg\ m^2$)
f_0	0.17	f_1	0.19×10^{-6}
ρ_{air}	1.18 (kg/m^3)	g	9.80 (m/s^2)

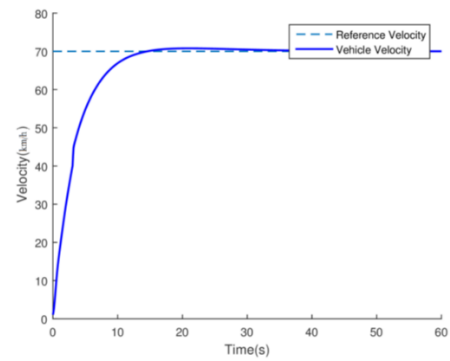


Figure 12. Velocity control relative to constant reference velocity

Controller output results for the reference input shown in of Figure 12, is in Figure 13.

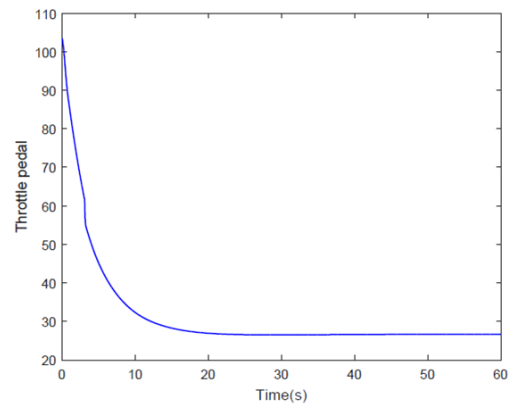


Figure 13. Control output for the reference velocity of 70 (km/h)

Changes in tuning parameters related to reference input shown in Figure 12, are in Figure 14.

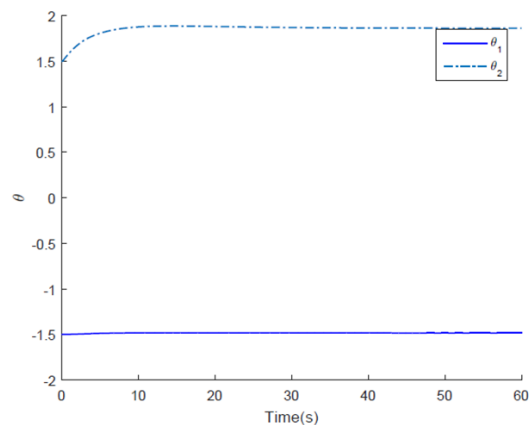


Figure 14. Changes of controller parameters vs. time

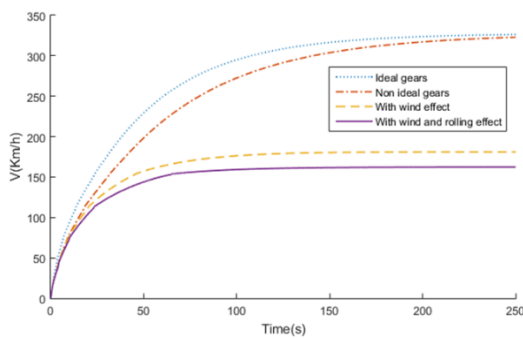


Figure 11. Simulations related to the importance of considering non-ideal gearbox, rolling resistance and air resistance

To show the effectiveness of the control system, a simulation with the desired speed of 70 (km/h) has been performed. The result of this simulation represented in Figure 12. As can be seen, the controller has made the vehicle reach the desired velocity.

Meanwhile, in another simulation, control of velocity has been attempt despite of variable reference velocity (Figure 15). The results of this simulation represented as follows (Figure 16).

Moreover, the speed of torque converter's sides has reported to show the differences in the speed of torque converter's sides (Figure 17).

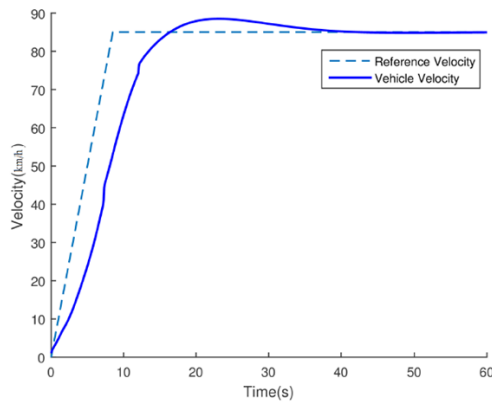


Figure 15. Portrayal of control system performance for variable reference velocity vs. time

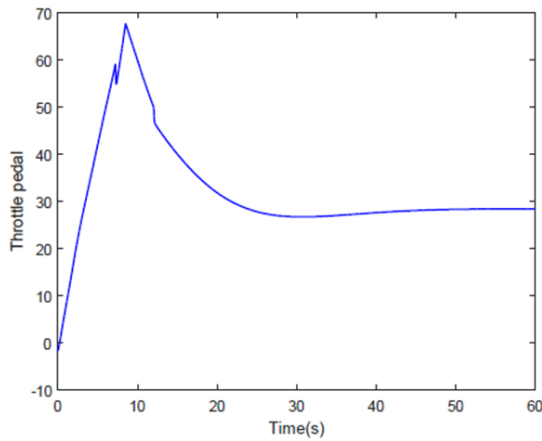


Figure 16. Control output (gas pedal) for tracking reference velocity

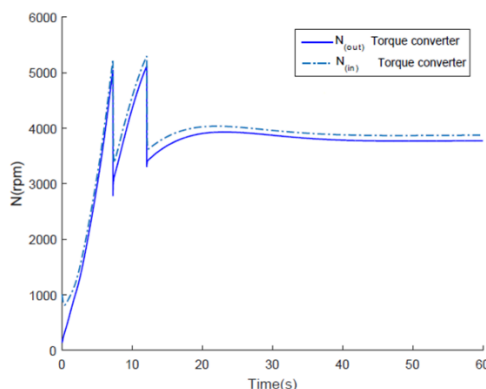


Figure 17. Portrayal of differences in the speed of torque converter's sides

As stated in the results section, assumptions such as rolling resistance, air resistance, a not ideal gearbox, the existence of a torque converter and an internal combustion engine, are of vital importance and must not neglect. In this study, the researchers described the importance of the aforementioned parameters while conducting comparative simulations. As it is mentioned in *equivalent mass and force* section, the defined forces (rolling force and aerodynamic force) and the behavior of internal combustion are non-linear that affects the velocity of the vehicle. Therefore, the researchers suggested a proper model reference adaptive controller for variability of nonlinear intelligent vehicle dynamics. To sum up, this research shows a breakthrough in controlling the longitudinal speed of intelligent vehicles by implementing MRAC on an intelligent highway.

Declaration of Conflicting Interests

The authors declared no potential conflicts of interest with respect to the research, authorship, and/or publication of this article.

References

[1] R. Jurgen, "Smart cars and highways go global," *IEEE Spectr.*, 1991.

[2] R. Fenton, "IVHS/AHS: Driving into the future," *IEEE Control Syst.*, 1994.

[3] P. Varaiya, "Smart cars on smart roads: problems of control," *IEEE Trans. Automat. Contr.*, 1993.

[4] R. Bishop, *Intelligent vehicle technology and trends*. 2005.

[5] M. Broucke and P. Varaiya, "The automated highway system: A transportation technology for the 21st century," *Control Eng. Pract.*, vol. 5, no. 11, pp. 1583–1590, Nov. 1997.

[6] K. Li and P. Ioannou, "Modeling of traffic flow of automated vehicles," *Trans. Intell. Transp. ...*, 2004.

[7] S. Tsugawa, S. Kato, and K. Tokuda, "A cooperative driving system with automated vehicles and inter-vehicle communications in Demo 2000," *Intelligent*, 2001.

[8] J. Luo and J. Hubaux, "A survey of research in inter-vehicle communications," *Embed. Secur. Cars*, 2006.

[9] T. Willke and P. Tientrakool, "A survey of inter-vehicle communication protocols and their applications," *Surv. Tutorials*, 2009.

6. Conclusion

- [10] Q. Xu, K. Hedrick, and R. Sengupta, "Effects of vehicle-vehicle/roadside-vehicle communication on adaptive cruise controlled highway systems," *Proceedings. VTC*, 2002.
- [11] U. Palmquist, "Intelligent cruise control and roadside information," *IEEE micro*, 1993.
- [12] D. Ngoduy, "Instability of cooperative adaptive cruise control traffic flow: A macroscopic approach," *Commun. Nonlinear Sci. Numer.*, 2013.
- [13] S. Yu and Z. Shi, "The effects of vehicular gap changes with memory on traffic flow in cooperative adaptive cruise control strategy," *Phys. A Stat. Mech. Its Appl.*, 2015.
- [14] L. Xiao, M. Wang, B. van Arem, L. Xiao, and M. Wang, "Realistic Car-Following Models for Microscopic Simulation of Adaptive and Cooperative Adaptive Cruise Control Vehicles," *Transp. Res. Board*, 2017.
- [15] C. Melson, M. Levin, and S. Boyles, "Modeling Cooperative Adaptive Cruise Control in Dynamic Traffic Assignment," *Transp. Res. Board*, 2017.
- [16] V. Milanés and S. Shladover, "Handling cut-in vehicles in strings of cooperative adaptive cruise control vehicles," *J. Intell. Transp.*, 2016.
- [17] L. Menhour, B. d'Andrea-Novell, M. Fliess, D. Gruyer, and H. Mounier, "An Efficient Model-Free Setting for Longitudinal and Lateral Vehicle Control: Validation Through the Interconnected Pro-SiVIC/RTMaps Prototyping Platform," *IEEE Trans. Intell. Transp. Syst.*, pp. 1–15, 2017.
- [18] H. Zhang and J. Wang, "Vehicle Lateral Dynamics Control Through AFS/DYC and Robust Gain-Scheduling Approach," *IEEE Trans. Veh. Technol.*, vol. 65, no. 1, pp. 489–494, Jan. 2016.
- [19] "SAE J670e," in *Automotive, Society of Engineers (SAE), Inc.*, Warrendale, PA.
- [20] R. Di Martino, "Modelling and Simulation of the Dynamic Behaviour of the Automobile," 2005.
- [21] S. SAE, "J2396 Surface Vehicle Recommended Practice, Definitions and Experimental Measures Related to the Specification of Driver Visual Behavior Using," 2000.
- [22] K. Åström and B. Wittenmark, *Adaptive control*. Dover Publication, 2013.

Appendix

Table 2: Internal engine output torque[20]

		Throttle in percent									
		0	20	30	40	50	60	70	80	85	100
Engine speed (RPM)	800	26.8204	145.1599	165.2752	177.0149	177.0149	179.0264	179.0264	179.0264	179.0264	179.0264
	1200	-29.5025	78.4498	139.4663	175.3328	187.0726	195.4482	199.1418	201.8238	201.8238	201.8238
	1600	-32.855	56.9934	119.3509	161.5931	189.0841	196.4597	205.5058	206.5174	209.1994	209.1994
	2000	-35.5371	45.2537	99.2356	146.8419	185.3905	199.1418	205.5058	209.1994	213.893	213.893
	2400	-38.2191	29.5025	81.8023	129.4086	175.3328	195.4482	205.5058	213.893	219.2571	219.2571
	2800	-40.9012	19.4448	69.7331	111.9753	159.5816	185.3905	201.8238	216.575	219.2571	223.9507
	3200	-43.5832	6.7051	56.9934	101.9177	149.5239	175.3328	196.4597	213.893	219.2571	223.9507
	3600	-46.9358	-1.341	45.2537	89.178	139.4663	171.6508	189.0841	211.8815	219.2571	223.9507
	5000	-49.6178	-8.7166	32.1845	79.7908	126.7266	156.8996	179.0264	199.1418	209.1994	213.893
	5400	-52.2999	-15.7512	22.1269	65.3691	115.6574	142.1483	166.9572	187.0726	196.4597	205.5058
5800	-55.9819	-21.4564	12.0692	56.9934	101.9177	129.4086	151.5355	169.6393	179.0264	185.3905	

In the Table 2, there are internal combustion engine information used in the article. The amount of torque produce in this kind of engines depends on the amount of opening throttle and the engine speed.

Verifications steps with CarSim software represented in the following figures. In Figure 18, ideal model without considering rolling and aerodynamic resistance shown. In Figure 19, not ideal gearbox added to the model and shown. Then, aerodynamic resistance implemented and represented in Figure 20. The final step, rolling resistance considered as well, and can be seen in Figure 21.

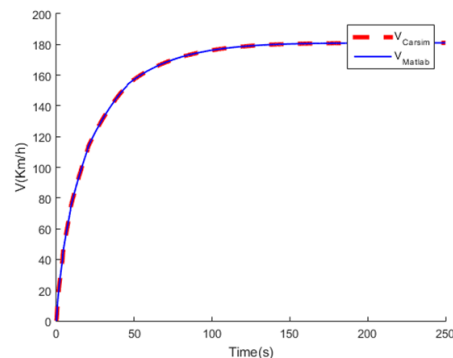


Figure 20. Implementing model with aerodynamic resistance and non-ideal gearbox.

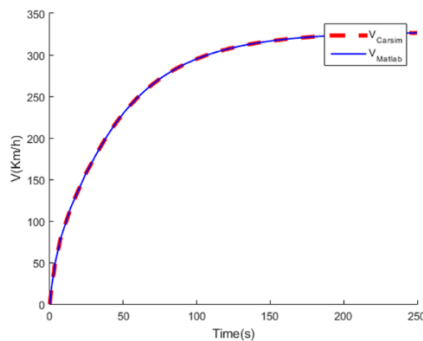


Figure 18. Ideal model with considering ideal gearbox.

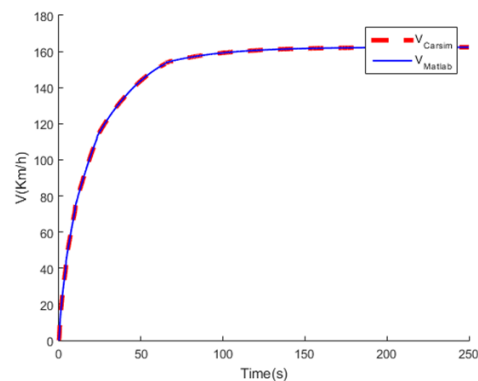


Figure 21. Implementing model with aerodynamic resistance and considering rolling resistance and non-ideal gearbox.

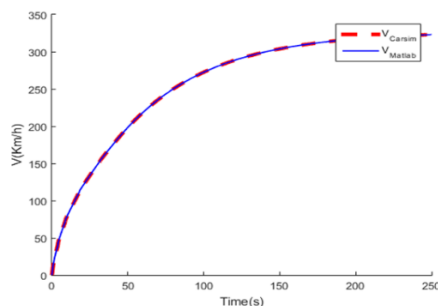


Figure 19. Ideal model with considering non-ideal gearbox.